Structure, Dynamics, and Reactions of Supercritical Water Studied by NMR and Computer Simulation

Masaru Nakahara

Division of Environmental Chemistry
Institute for Chemical Research, Kyoto University, Kyoto 611-0011, Japan

E-mail: nakahara@scl.kyoto-u.ac.jp

The structure and properties of supercritical water is investigated in relation to the energy and environmental issues of the 21st century. Molecular interpretations are given to the temperature dependence of the hydrogen-bonding structure, dynamics, and chemical reactions of supercritical water. The three-dimensional network structure, characteristic of ambient water, is broken down in hot expanded water at temperatures higher than ~200 ˚C and densities lower than ~0.9 g cm^{-3}. The number of hydrogen bonds per molecule has been determined by the NMR method combined with computer simulation; it decreases from ~4 for ambient water to 1-2 for supercritical water at 400 ˚C and the critical density (~0.32 g cm^{-3}). The NMR rotational correlation time (τ_{2R}) for supercritical water at the medium densities is in the range of 50-70 fs, two orders of magnitude smaller than the ambient value. New hydrothermal organic reactions without catalyst are developed for green chemistry. In hot water, carbon monoxide, carbon dioxide, and hydrogen are linked through formic acid. Formic acid can serve as a chemical tank for the compact transportation and storage in the clean hydrogen fuel technology.

1. Introduction

Water is one of the most important substances for all of us, the livings on Earth. Water has been attracting many people over a wide range from the ancient to the present. Its great needs and usefulness attract engineers, scientists, and common people. Its unique and miraculous properties fascinate scientists, engineers, and common people. In recent years, attention is paid to water at high temperatures and pressures from the fundamental and application viewpoints. To increase the efficiency of energy conversion to electricity from chemical bonds or nuclear states, the temperature and pressure of steam used in the power generation get higher and higher. Thus we need to observe and understand a variety of properties of supercritical water; here supercritical water is defined rather widely as water at temperatures higher than the critical temperature, 374 ˚C.

Supercritical water attracts many scientists and engineers as a clean reaction medium alternative to hazardous organic solvents. Nonpolar organic compounds, which are insoluble or sparingly soluble in ambient water, become completely miscible in high-temperature and high-pressure water. Thus new unusual organic reactions can take place in hot water. One may ask the following questions: (i) why does the solubility of organics increase, (ii) why can new reaction pathways be opened by supercritical water, (iii) how are reactions controlled by the supercritical water solvation for the chemical species involved in reactions, reactants, intermediates, and products. For a better understanding of supercritical water chemistry, we need to develop new experimental and theoretical methods. It is shown here how powerful high-temperature NMR spectroscopy is in the study of microscopic properties of hot water. The energy-representation method has been developed for liquid theory and applied to the determination of solvation free energies for inorganic and organic species in hot water. Advances in science and technology must be in harmony with the welfare of the human beings. This is true also in the case of our study on supercritical water. Many chemical and physical problems to meet in power cycle technology can be solved with the aid of chemists, physicists, and materials scientists. Knowledge of chemistry and

physics of supercritical water is also necessary for a deeper understanding of geophysical issues.

Human beings are confronted with the energy and environmental problems in the 21st century. The Kyoto protocol, which was adopted here at the third Conference of the Parties to the United Nations Framework Convention on Climate Change in Kyoto in December 1997, sets numerical targets for curbing emissions of carbon dioxide and other greenhouse gases; the natural gases should not be lost into the atmosphere because they have one order of magnitude larger greenhouse effect factors. It is thus hoped to plan our daily life and industrial production activities in harmony with Earth environments. On one hand, the increasing rate of the energy demand does not stop but rather increases because the people want to improve the welfare, and because the world population "explosively" increases. On the other hand, energy should be consumed under the conditions of environmental protection. We are not allowed to exhaust fossil fuels in very near future.

Human beings are in a dilemma about whether to go or not. We should find a solution to the global energy and environmental issues for the sustainable development of our welfare. We should develop knowledge about scientific and industrial methods for new clean energy resources like hydrogen [1] and the alternative (LNG, DME) [2] as recently reviewed [3-5]. At the same time, we are urged to innovate efficient ways of treating water and aqueous solutions in the application areas, say, in the power cycle technology. To make the water treatment more efficient and safer, we need to carry out underlying fundamental researches on water and aqueous solutions. Electricity generation relies upon the large-scale treatment of water over a wide range of temperature and pressure. Thus interplay between science and technology of water is desirable and discussed in the 14th ICPWS in the place where the Kyoto protocol was adopted.

To achieve a higher efficiency in the power plant, it is insufficient to control such macroscopic properties of water as the *p-V-T* relation, dielectric constant, viscosity, autoprotolysis constant, and so on. For better understanding and control of chemical reaction processes taking place in aqueous systems, it is necessary to obtain deep insights into the microscopic or molecular-level properties, such as the structure, dynamics and reactions. Physical chemistry of water and aqueous solutions should provide a backup or feedback to make more reliable and powerful the practical power cycle chemistry.

Thermodynamic properties of water have been very accurately evaluated and accumulated over a wide range of thermodynamic states by the leading role played by IAPWS (The International Association of the Properties of Water and Steam); the recommended data are available in the website (http://www.iapws.org/) and also contained in the CD-ROM attached as an appendix of the present proceedings of the 14th ICPWS. There remain more chemical reaction problems to be solved from microscopic viewpoints.

2. Electrolyte Conductivity

For the past decades, we have investigated a variety of ionic solutions under extreme conditions by applying conductivity method [6-25]. For scientific and technological purposes, electrical conductivity is measured in many situations using a conductivity cell that can stand against extreme conditions. Conductivity is a dynamic response to the application of electric field to the ionic species in solution and can provide us with information on the ion mobility at infinite dilution and ion association as a function of electrolyte concentration.

Mobility of the free ion in ambient water has often been interpreted in terms of a hydrodynamic continuum (Stokes-Einstein-Debye) model where the viscosity represents the role of solvent; the ionic charge is taken into account in the driving force but neglected in the treatment of solute-solvent interactions. This has been improved by the Hubbard-Onsager (HO) dielectric friction theory that has taken into account the role of the ionic hydration dynamics through the solvent dielectric relaxation delayed by ionic movement on the primitive level. We have tested the applicability and limitations of the HO theory over a wide range of thermodynamic conditions; for detail, see the original papers [14-19, 21-25].

One of the technical merits of conductivity measurements is a high sensitivity with a high cost performance. The accuracy depends on the cell constant and the solvent blank conductivity to be subtracted. It is desirable that the distance and areas of the electrodes are invariant over a wide range of measurement conditions. When it is varied, a correction is to be made. Electrolyte conductance in aqueous system is obtained by subtracting the water conductivity from the total solution conductivity; the degree of solvent correction increases with decreasing electrolyte concentration.

The solvent correction becomes significant in aqueous electrolyte solutions, in particular, at high temperatures including the supercritical; in the region near or over the critical conditions, both the total and solvent conductivities begin to drop due to the electrolyte association and water deionization (proton-hydroxide association). In consequence, the experimental errors increase at high temperatures, making the association constant involved in a conductance equation highly uncertain. Materials used for the conductance cell are expanded to change the cell constant; so far, there are no good ways for the calibration. These are discussed elsewhere [24, 25].

Other independent approaches are required to check the reliability and limitations of the conductivity method applied for the study of electrolytes at high temperatures. One is the MD (molecular dynamics) simulation, the so-called computer experiment and the other the NMR diffusion method.

When several pairs of ions are contained and interaction potentials are reliably treated in a water box of a reasonable size, MD simulation can yield a reasonable value of ionic self-diffusion constant or mobility. One of the important problems is how ionic mobility depends on the density of supercritical water. The MD simulation shows a rather monotonous dependency; see Ref. [26] and references cited therein. Experimental results however suggest the presence of a plateau or maximum before the mobility rise due to the gas-like behavior; note an increase in experimental error as mentioned above [24, 25]. It is interesting to compare the ion mobility determined with that by the pulsed-field gradient spin echo NMR method. In the case of NMR, drift of ions with a nuclear spin is driven by the externally applied magnetic field. There must be some differences in the mechanism between NMR and electric conductivity because magnetically specified ions migrate without the movement of counter-ions magnetically not tagged (not resonated). We can make such a challenging study on the fundamental mechanism. It is now in progress in our laboratory.

3. High-Temperature NMR Probe

Spectroscopic approach enables us to identify and quantify individual chemical species of interest irrespective of the presence of the charge as a function of frequency or energy. In this sense, nuclear magnetic resonance (NMR) spectroscopy is more informative than electric conductivity. Here we describe in brief the features of the high-temperature NMR probe used in the first

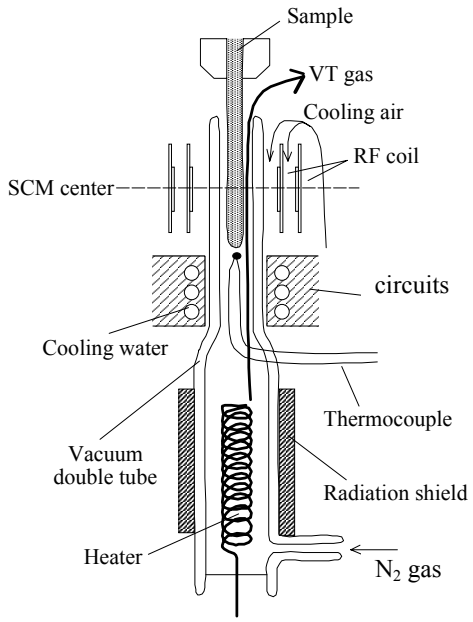

Fig. 1. Overview of the high-temperature probe.

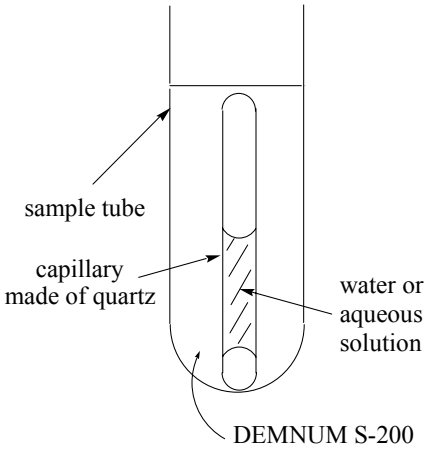

Fig. 2. Schematic view of the sample setup.

observation of the proton chemical shift in supercritical water [27, 28].

When water is heated in a closed vessel up to temperatures higher than 374 °C, liquid water transitions to supercritical water; the pressure is dependent on the filling factor that is defined by the volume of ambient water divided by that of the vessel. When the filling factor is numerically equal to the critical density (0.32 g/cm^3), the pressure at the critical temperature is 22 MPa. Supercritical water thus prepared is at high temperature and high pressure. We have carried out the NMR experiment on supercritical water by using a high-temperature probe shown here. Water is confined in a quartz capillary placed in an NMR sample tube and a high pressure is achieved by raising the temperature of the capillary in a way described below.

We have been developing a high-temperature NMR probe in cooperation with an instrument company (JEOL). In Fig. 1 there is shown an overview of the first-generation high-temperature probe. The sample is heated up by heated nitrogen gas passed along the sample tube; the gas is heated in the lower compartment by an electric heater before it is introduced to the upper region. We have insulated the RF coil and the detection circuits by a vacuum double tube made of quartz. Cooling air and cooling water also circulate around the RF coil and the detection circuits, respectively, in order to keep their temperatures constant. The radiation from the heater coil is shielded by equipping a radiation shield around the heater. Since the temperature is raised only for the sample system, the coil and detection systems are protected and their performance does not deteriorate with an increase in the sample temperature.

Recently, we have drastically changed the design shown in Fig. 1 and succeeded in developing the third-generation high-temperature probe [29]. In the improved probe, there are upper and lower heaters arranged symmetrically with respect to the sample or RF center. No gas is used and the heating system is composed of solid materials. In particular, a tube holder is made of ceramic with a high thermal conductivity and fixed to the heaters; the thermal conductivity is on the order of that of copper. The new type probe is tunable, and the multinuclear measurement is now possible without remounting the sample tube. Furthermore, the new probe is equipped with a magnetic field gradient coil. The maximum strength of the field gradient is as large as 250 G/cm, and the probe is a powerful apparatus for multinuclear measurements of self-diffusion constants for a variety of ionic and nonionic species. The gas flow is not used any more, and the heaters give a high and stable temperature atmosphere through conducting Au. The homogeneity of the temperature is dramatically improved so that the inhomogeneity is ~1 °C in the RF observation area, while the first-generation probe involves a temperature inhomogeneity of ~5 °C. The results presented in this paper are taken by using the probe illustrated in Fig. 1. The work using the new probe is now in progress to investigate hydration structure and dynamics of supercritical aqueous solutions of electrolytes. Preliminary results were reported recently [30].

Figure 2 shows a schematic view of the sample setup. The sample fluid is confined in a sealed capillary made of quartz. The sample capillary is put into the NMR sample tube. We use a fluorinated oil free of hydrogen atoms, DEMNUM S-200 (Daikin Co.). This is a heat medium useful even at a temperature of 400 °C or higher. Any reference material does not need to be sealed by correcting the magnetic susceptibility directly; for a detail, see the reference [27, 28]. The state of water in a sealed capillary is determined from the phase diagram and the equation of state (IAPWS-SF95 and IAPWS-IF97). In our sample setup, the liquid and gas phases coexist up to the transition temperature T_t and the distinction between the liquid and gas phases disappears at T_t, which is uniquely determined by the content of water in the capillary. When the temperature is raised beyond T_t, the water in the capillary is in the one-phase region. In this region, since the volume of the capillary is constant, the density of water remains constant against the change in the temperature. Thus, at a temperature above T_t, the temperature and density can be controlled as independent variables in the capillary method. At a temperature below T_t, on the other hand, since the water in the capillary is in the two-phase region, only the temperature can be controlled independently. The densities of the liquid and gas phases are given by the saturation curve (IAPWS).

4. Intermolecular Potential Functions

In principle, the properties and structure of water under any thermodynamic conditions can be determined by intermolecular interactions scaled by the thermal energy $k_B T$ as the Boltzmann factor.

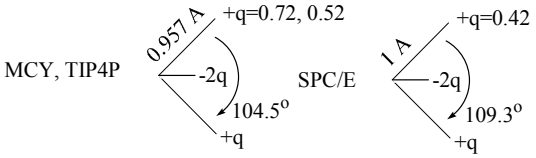

Fig. 3. The location and magnitude of the partial charges allotted on each atom in water model. The charge q is given in the unit of e.

The pair-wise additivity is the most often used approximation for the interaction potential energy; relevant references are shown in the review article [31]. Stillinger and Ben-Naim have developed a simple potential form, called ST2. This is a four-point-charge model with the T_d symmetry. It has been used widely to reproduce characteristic features of ambient water. Since the parameters of the ST2 potentially are determined so that some of thermodynamic properties may be reproduced by the potential. To overcome the limitations due to the empiricism, some other potential functions have been derived according to quantum mechanical calculations. Matsuoka, Clementi, and Yoshimine have computed quantum mechanically intermolecular interaction energies with many different configurations and have fitted into a functional form with many parameters; this is designated as MCY. Following the significance of the quantum mechanical origin, simpler effective pair potentials are developed after MCY. They are TIP4P, SPC, and SPC/E.

The quantum mechanics-based potential function U between a pair of i and j molecules is approximately expressed as,

$$U(r_{ij}) = U_{LJ} + U_C \quad (1)$$

where U_{LJ} and U_C denote the Lennard-Jones (LJ) and Coulombic parts of the potential, respectively. The important point is that the negative charge is located between the oxygen and the hydrogen atoms but not on the other side of the O-H bonds. The Lennard-Jones potential is taken into account only for the oxygen-oxygen pair. Thus the hydrogen-bonding interaction is simplified, and there is no requirement of such a switching function as that used in ST2.

The second term U_C in Eq. 1 plays a key role in controlling in a mimic way the hydrogen-bond formation in water. It is to be noted that the partial changes used for the hydrogen atom is close to or even larger than $0.5e$ (e, the elementary charge), and the partial charge allotted to the oxygen atom is close to $-e$ or even more negative than the univalent anion as shown in Fig. 3. Although the water molecule itself is neutral when it is viewed from a long distance, the electrostatic field in the vicinity of the constituent atoms is remarkably large with the short-range field strength similar to that of relatively large univalent ions. The strong fields due to the positive and negative charges are considerably cancelled at high molecular packing densities. This is the case for ambient water. When water is expanded with increasing temperature, however, the local field cancellation due to the overlapping decreases as the packing density is lowered. This is the case for hot water including the supercritical.

Hot water under supercritical conditions is significantly expanded and thermally stretched. Hot

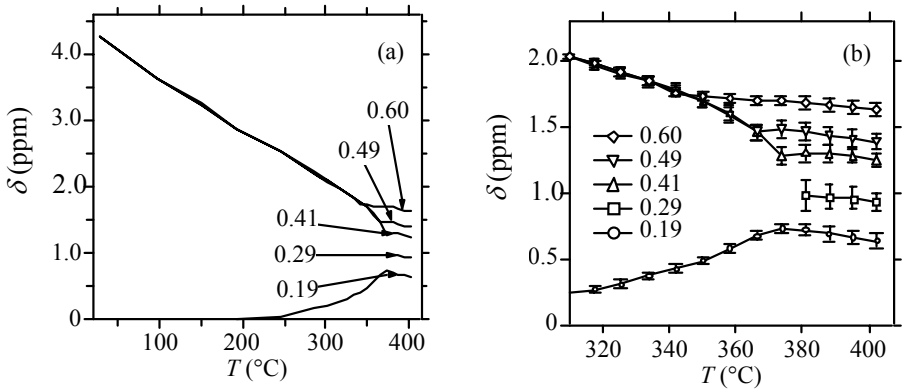

Fig. 4. (a) Water proton chemical shifts δ plotted against the temperature T. The numbers in the figures represent the density of water in the one-phase region expressed in the unit of g/cm^3. At subcritical temperatures, the two values of the chemical shift are obtained from the gas and liquid phases of the saturation curve. (b) Expanded plot of the high-temperature region in (a).

water is thus less packed than ambient water. The resulting electric molecular field fluctuates strongly and anisotropically due to more or less naked water partial charges at high temperatures and low packing densities. Thus the molecular packing density and charge field are locally fluctuating to a large extent in a long range; this is called microheterogeneity. Hot water, expanded and rapidly fluctuating in the density, can accommodate both polar and nonpolar molecules in the vacancies and results in the entropy production. This is one of the reasons for the increase of the solubility of nonpolar molecules.

It is interesting to see how much the effective potentials can reproduce anomalous properties of ambient water, such as the temperature of the maximum density, the temperature of the minimum expansivity and compressibility. Despite the simplicity, the three-point-charge models, SPC and SPC/E, can reproduce the thermodynamic anomalies and the radial distribution function as well. The SPC/E potential model is widely used for supercritical water.

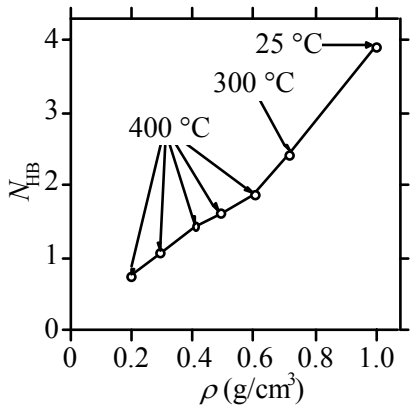

Fig. 5. The average number N_{HB} of hydrogen bonds in which a water molecule is involved. The quantity ρ stands for the density of water.

5. Structure of Hydrogen Bonds

The hydrogen-bonding structure of water can be probed by the proton chemical shift [27, 28]. In Fig. 4(a), we show the chemical shift δ as a function of the temperature T. The δ value is referenced to the water molecule at isolation, so that δ is a measure of the interaction strength of a water molecule with the surroundings. Note that there are two values of δ at each temperature when the system is in the two-phase region (on the liquid-gas saturation curve). In the two-phase region, the curve in Fig. 4(a) with the lower-field values of δ represents the chemical shift of water in the liquid phase and the curve with the higher-field values corresponds to the gas phase. When the temperature is above T_t, where water is in the one-phase region, the chemical shift is a function of both the temperature T and the density ρ. The chemical shift δ in the super- and subcritical regions is shown in Fig. 4(b). According to Fig. 4(b), the chemical shift increases with the density at each temperature above the critical one, and it decreases with the temperature at constant density. It should be noted, in addition, that the temperature dependence of the chemical shift is apparently smaller at high temperatures than at ambient conditions.

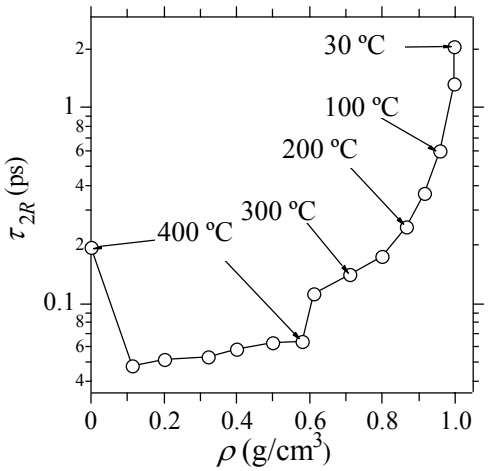

Fig. 6. The reorientational correlation time τ_{2R} of heavy water as a function of the density ρ. The quantity ρ is converted to the corresponding mass density of H_2O in the unit of g/cm^3.

The key point of Fig. 4 is that the chemical shift δ is not zero even under supercritical conditions. This evidences that the hydrogen bonding persists in supercritical water. The hydrogen-bonding state of supercritical water was an issue of debate since a neutron scattering group claimed the absence of the hydrogen bonding [32]. Figure 4 concludes the issue in favor of the presence of the hydrogen bonding. The NMR study combined with computer simulation clarifies that supercritical water is a hydrogen bonding solvent [27, 28, 33].

The hydrogen bonding of water is not an "all-or-none" type of quantity, however. Its characterization needs to be completed with a quantitative analysis within a well-defined framework. For this purpose, we converted the chemical shift δ into a conceptually more insightful and convenient quantity through computer simulation. From a set of computer simulations, we showed that δ of super- and subcritical water is proportional to the average number of hydrogen bonds N_{HB}, which is defined as the integral value of the intermolecular O-H radial distribution function g_{OH} up to a certain cut-off distance r_c. In Fig. 4, we show N_{HB} as a function of the density ρ at a typical value 2.4 Å as r_c. It is evident that when the density is larger than the critical one, a water molecule is involved in at least one hydrogen bond. Our NMR results on the water proton chemical shifts are in good agreement with those obtained almost at the same time [34].

Recently, Takebayashi et al. have investigated the hydration of acetone in supercritical water by ^{13}C NMR using the same NMR method [35]. The chemical shift of the carbonyl carbon of acetone is dependent on the temperature and water density in a way similar to those in Fig. 4. The common features are understandable in the sense that the carbonyl group is strongly polarized and can be hydrogen-bonded to neighboring water molecules.

6. Rotational Dynamics

The chemical shift studies inform us of a hydrogen-bonding structure averaged over various hydrogen bonding states. In order to understand how chemical reactions are controlled by hydrogen-bonding interactions, we have carried out the dynamical studies that characterize the dynamic aspect of interconversion among the microscopic states; we have applied both NMR spectroscopy and computer simulation [36]. In particular, the intermolecular interaction of such a hydrogen bonding fluid like water is strongly dependent on the orientation of the molecules involved, and the rotational dynamics can be more suited to probe the local structure of fluid than the translational dynamics that can be more long-ranged. Following the chemical shift measurements described in the previous section, we determine the reorientational correlation time of a water molecule in supercritical conditions by measuring the deuteron NMR spin-lattice relaxation time (T_1).

We have carried out the T_1 measurements by using heavy water (D_2O). It is possible to show that unlike T_1 of H_2O, T_1 of D_2O is governed by the quadrupolar mechanism. The value of T_1 of D_2O then provides the second-rank reorientational correlation time τ_{2R} of a single water molecule. In Fig. 6, we show τ_{2R} as a function of the density ρ, where ρ of D_2O is expressed as the corresponding mass density of H_2O in the unit of g/cm^3. It is seen that τ_{2R} decreases rapidly with the temperature on the liquid branch of the saturation curve. While the reorientational relaxation proceeds on the order of picosecond (ps) in ambient water, it does on the order of several tens of femtoseconds (fs) when a supercritical state is realized.

The density dependence of τ_{2R} in supercritical conditions (400 °C) presented in Fig. 6 is weak compared to that of the chemical shift shown in Fig. 4. Actually, the value of τ_{2R} changes only by a factor of ~1.2 in response to the unit variation of the number of hydrogen bonds in Fig. 5. The rotational dynamics reflects only weakly the change in the state of the hydrogen bonding caused by the density variation. The weaker density dependence of an orientational degree of freedom is also observed in the context of the equilibrium structure. It was shown that while the radial distribution function of supercritical water involves a higher peak at a lower density, the orientational distribution function is essentially independent of the density variation at a fixed supercritical temperature [33].

While τ_{2R} is the relaxation time of an orientational degree of freedom in the coordinate space, the relaxation in the momentum space is characterized by the relaxation time τ_J of the angular momentum. τ_J of supercritical water was measured previously [37]. The relation $\tau_J > \tau_{2R}$ holds over the entire range of supercritical conditions examined. Thus, the reorientational relaxation of supercritical water is not diffusive and the inertial effect is operative. Indeed, the density dependence at 400 °C is larger in the order of 1) diffusion constant, 2) viscosity, and 3) τ_{2R}. The difference in the strength of the density dependence is actually 4-fold between the diffusion constant and τ_{2R}, in agreement with the above observation that the orientational degree of freedom is weakly influenced by density variation.

In Fig. 6, τ_{2R} exhibits an inversion of the τ_{2R} dependence in the low-density regime. In principle,

the reorientational correlation time τ_{2R} is to diverge in the limit of zero density because the angular momentum of each molecule is conserved when the intermolecular interactions are absent. Fig. 5 thus shows that the water molecule becomes "free" when the density is reduced below ~1/3 of the critical one.

7. Noncatalytic Hydrothermal Reactions

Water used for the power cycle is highly purified to avoid chemical troubles induced by the surface and bulk interactions with metals or metal ions. However, simple organic and inorganic compounds can contaminate water. Impurity compounds can be accumulated in the cracks in walls because a huge amount of water is used in a cyclic manner. In order to find what species are responsible for the corrosions, we need a new textbook on organic and inorganic reactions in hot water for the power cycle chemistry; chemistry is required as well as materials science and mechanical engineering. In order to establish the hydrothermal chemistry for the next generation, systematic studies on the reaction of each functional group is necessary in manner friendly to Earth. To elucidate the detailed pathways, kinetics, and mechanism, it is necessary to quantitatively analyze all products, intermediates, and reactant including the volatile im ambient conditions. We can apply the powerful NMR method for the total and detailed analysis of the chemical involved in the reaction. We can do the ^{1}H and ^{13}C elemental analysis even for the volatile [38].

7.1. Effective Acid Character of Hot Water

Hot water has attracted much attention recently as a novel solvent for chemical processes of synthetic, environmental, or geological importance and as an environmentally friendly alternative to harmful organic solvents. Unlike ambient water, water under hydrothermal conditions mixes well with organic compounds. It also acts as a noncatalytic medium to often induce a chemical reaction that does not proceed without acidic or basic catalysts on a practically accessible time scale under ambient conditions. The noncatalytic reactivity in water under hydrothermal conditions is often presumed to be a catalytic effect of H^+ or OH^- produced by the autoprotolysis of water. Indeed, the ion product of water increases with the change of the thermodynamic state from ambient to hydrothermal, and $[H^+]$ and $[OH^-]$ grow correspondingly by one to two orders of magnitude (IAPWS). On the other hand, the reaction rate constant is generally a strong function of the thermodynamics state, and $[H^+]$ or $[OH^-]$ may not be the sole factor to govern the reaction rate variation upon temperature elevation. Thus, quantitative kinetic measurements are necessary to examine the role of H^+ or OH^- in a noncatalytic reaction in hot water. In this section, we focus on a model ether reaction under hydrothermal conditions, and clarify the contribution of H^+ in the noncatalytic kinetics [39].

The model chemical reaction treated in the present work is the conversion between 1,4-butanediol and tetrahydrofuran (THF). The forward reaction is dehydration and the backward one hydrolysis. This reaction is a simplest reaction involving ether bonding. The ether bonding is a building component of coal, starch, and cellulose, and its reaction under hydrothermal conditions is important from energy and food concerns. Furthermore, the dehydration process is of synthetic utility for preparing an industrially important solvent, THF. Under ambient conditions, it is well known that both the forward and backward reactions need acid or metal catalysts. In hot water, it is observed that the reaction proceeds even without catalysts. No byproducts were detected and the reversibility was attained. Our purpose is to perform detailed kinetic analyses on the model conversion reaction given between 1,4-butanediol and THF, rather than to add another example of noncatalytic reaction in hot water.

Our kinetic analysis is based on a general expression for the reaction rate constant of an acid-catalyzed reaction. When the concentration of the oxonium ion is expressed as $[H^+]$, the observed rate constant k_{obs} is given by

$$k_{obs} = k_{water} + k_{acid}[H^+] \quad (2)$$

where k_{water} is the first-order rate constant under the hypothetical condition that H^+ is absent in the aqueous system, and k_{acid} is the second-order rate constant in the presence of H^+. It should be emphasized that k_{water} is the limiting intercept in Eq. 2. Since H^+ is always present due to the autoprotolysis of water, $[H^+] = 0$ needs to be hypothetically set to define k_{water}. In the following, k_{water} and k_{acid} are called the water-induced and acid-catalyzed rate constants, respectively. In a typical acid-catalyzed reaction at room temperature, k_{water} is too small to be detected on the practical time scale of seconds to days. In this case, k_{obs} is dominated by the second term of Eq. 2 and appears

to be proportional to $[H^+]$. In contrast, when the undissociated form of water becomes kinetically manifest on a practically accessible time scale, the water-induced term k_{water} will be appreciably different from zero. A nonzero intercept is to be revealed in the plot of k_{obs} against $[H^+]$. On the basis of this idea, we determine both k_{water} and k_{acid} by varying $[H^+]$ in the low-concentration range. The role of water as a solvent can then be clarified by decomposing k_{obs} into the k_{water} and k_{acid} terms at neutral (nonacidic) conditions, where no acid is added from outside and H^+ is present only by the autoprotolysis of water.

Suppose in Eq. 1 that k_{water} is negligible compared to $k_{acid}[H^+]$ in the experimental range of $[H^+]$. Under this supposition, since the ionization of the water molecule gives rise to 10^{-6} M of the oxonium ion at 270 °C in the neutral condition, for example, the addition of 10^{-4} M (M = mol/dm^3) HCl is to increase k_{obs} by two orders of magnitude. Figure 7(a) then illustrates the experimentally determined dependence of k_{obs} on $[H^+]$ for the dehydration of 1,4-butanediol to THF at temperatures of 150 and 270 °C on the water saturation curve. Evidently, k_{obs} in the $[H^+]$ range of ~10^{-4} M is only 2 or 3 times as large as k_{obs} at the neutral condition. In other words, the intercept in the $[H^+]$ dependence of k_{obs} is evidently nonzero under our experimental conditions. Figure 7(b) shows the $[H^+]$ dependence of k_{obs} at a supercritical state of 400 °C and 0.4 g/cm^3 In this case, HCl is only weakly dissociated and $[H^+]$ was evaluated from the ionization constant of HCl listed in a literature [40]. The presence of a nonzero intercept is also evident in Fig. 7(b). According to the values of k_{water} and k_{acid} determined from Eq. 1, $k_{acid}[H^+]$ is found to contribute by less than ~5% to k_{obs} in the neutral condition. Therefore, Fig. 6 demonstrates in super- and subcritical conditions that water accelerates the reaction even without the presence of H^+. Moreover, we confirmed that the reaction does not proceed appreciably in the dilute gas condition even at high experimental temperatures of 350 and 400 °C. This shows that 1,4-butanediol does not dehydrate only by heat. The presence of the aqueous medium is necessary for dehydration. Water is thus revealed, at the level of kinetics, to promote the reaction in its undissociated form.

7.2. Elementary Reactions in Hot Water

To control hydrothermal reactions of a variety of organics in an earth-friendly manner, we need a systematic investigation on each functional group. Among the functional groups, aldehyde is important in laboratorial and industrial processes as solvent and synthetic starting material. In this section, we introduce the general reaction behavior of aldehyde in hot water and point out the important role played by formic acid. What we have found for a new textbook are: 1) hydrothermal noncatalytic

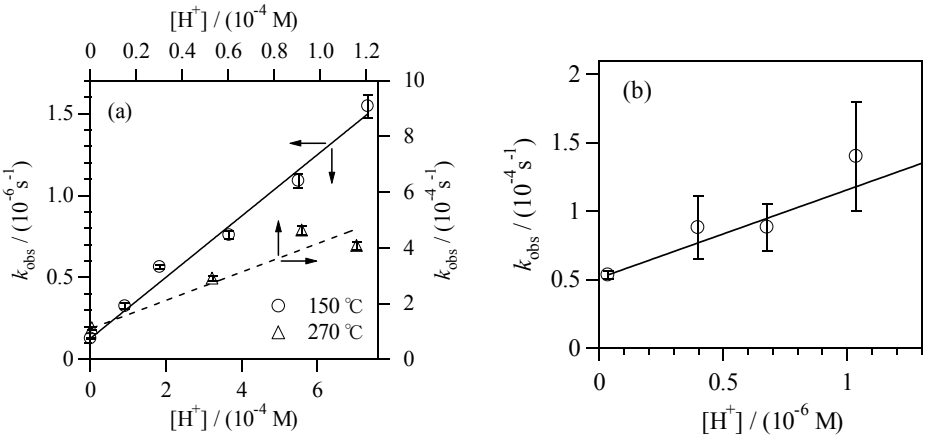

Fig. 7. The observed rate constant k_{obs} for the dehydration of 1,4-butanediol as a function of the oxonium ion concentration $[H^+]$ (a) at temperatures of 150 and 270 °C on the liquid branch of the water saturation curve and (b) at a supercritical state of 400 °C and 0.4 g/cm^3. The data at nearly zero $[H^+]$ correspond to the neutral (nonacidic) condition and $[H^+]$ is not exactly zero due to the autoprotolysis of water. The linear fits are shown by the lines.

self- and cross disproportionations forming alcohol and acid and 2) hydrothermal noncatalytic decarbonylation. All of the new reactions can be accelerated by the catalytic action of the metal surface heated up to the supercritical conditions of water. Power cycle chemists should pay attention to the features of chemical reaction pathways unveiled by fundamental research.

In ambient conditions, aldehyde exhibits the Cannizzaro (disproportionation) reaction; it takes places only in the presence of a large amount of base catalyst when α-hydrogen is absent. In hot water, the reaction behavior of an aldehyde is rich and rather complex even without catalysts. When a single type of aldehyde is dissolved in supercritical water, two types of disproportionation reactions actually occur without adding catalysts from outside. One of the disproportionation reactions is the self one. In the self-disproportionation, the aldehyde reacts in and with water through

$$2\ \text{R-CHO} + \text{H}_2\text{O} \rightarrow \text{R-CH}_2\text{OH} + \text{R-COOH} \quad (3)$$

In this reaction, alcohol and acid are produced at the ratio of 1:1. The reaction proceeds even when α-hydrogen is present; this is in contrast the description in the standard textbook. The other type of disproportionation is between the original aldehyde and formic acid. Formic acid is generated through the thermal decarbonylation of the aldehyde; carbon monoxide is generated as a decomposition product and reacts with water to produce formic acid. The scheme is given by

$$\text{R-CHO} + \text{HO-CHO} + \text{H}_2\text{O} \rightarrow \text{R-CH}_2\text{OH} + \text{H}_2\text{CO}_3 \quad (4)$$

Note that formic acid is "hydroxy aldehyde." According to the above scheme of the aldehyde in hot water, the alcohol is produced in excess to the acid. We have demonstrated the generality of the above scheme using form-, aceto-, and benzaldehydes [38, 41-43]. It was actually found that the cross-disproportionation involves a larger path weight than the self. In addition, the reaction of formaldehyde and formic acid was shown to lead in the presence of acid to the formation of a carbon-carbon bond in glycolic acid [44, 45]. This is a chemical evolution process from C1 (carbon one) compounds to a C2 compound. Glycolic acid can actually be aminated to provide glycine, the simplest member of amino acid.

Our finding concerning aldehyde points out the key role of formic acid played in hydrothermal reaction as shown below.

In addition to the reaction referred to above, aldehye undergoes the following reactions:

$$\text{R-CHO} \rightarrow \text{R-H} + \text{CO} \quad (5)$$

$$\text{CO} + \text{H}_2\text{O} \rightarrow \text{HCOOH} \quad (6)$$

At high temperatures, aldehyde shows the proton-transferred decarbonylation, Eq. 5 [38]. As a result, formic acid (hydroxyl aldehyde) is formed through the transformation of CO. As shown previously [1], formic acid decomposes into carbon dioxide and hydrogen. In consequence we can prepare hydrogen from the water-gas-shift reaction and formic acid can be used as a chemical tank for the compact transportation and storage [1].

Formic acid is a simple organic compound involving only one carbon atom. The chemistry of organics with a single carbon atom is called the C1 chemistry. An intensive study of the hydrothermal C1 chemistry is now in progress. Especially, we found that in mild hydrothermal conditions, glycolic acid is
synthesized from formaldehyde [44, 45]. This is a chemical evolution process from a C1 compound to a C2. The point is that a chemical evolution path is made a major one through a simple control of the reaction conditions; in this case, the increase of the concentration of formic acid. The reaction of open ethers (diethyl ether [46]; dimethyl ether, DME [2]) have been shown to have a new reaction process named proton-transferred fragmentation. Unexpectedly, the fragmentation process yields aldehyde and hydrocarbon. Main products of the

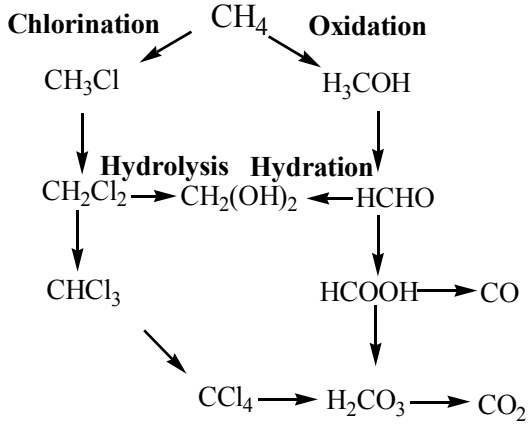

Fig. 8. Chlorination-oxidation-reduction C1 cycle starting with methane. Arrows are directed toward oxidation; the opposite direction (not shown) means the reduction. Water H_2O (not shown) plays a key role in controlling the hydrothermal C1 processes. Formic acid, carbon monoxide, and carbon dioxide can be mutually converted in the water-gas-shift reaction.

DME reaction in supercritical water are methane and methanol, both being important as fuels. This is the reason why we have extensively studied hydrothermal processes of aldehydes.

DME and formic acid can serve as a chemical tank for methane and hydrogen, respectively. Their liquefaction temperatures are rather close to room temperature. Therefore, it does not cost to transport and store in a vessel at temperatures near room temperature. Although hydrogen is an ultimately clean fuel, it must be compressed or absorbed in some materials for compaction.

Toward the understanding of the reaction mechanism in hydrothermal conditions, the role of water needs to be elucidated quantitatively through a molecular theory of hydration. For this purpose, we formulated the method of energy representation and analyzed the hydration behavior in hot water in strong connection to the solvation free energy for a variety of the chemical species and simple C1 reactions in hot water [47-51]. It has been shown how the solvation free energies for water, carbon monoxide, carbon dioxide, hydrogen, and formic acid (see Fig. 8) controls the water-gas-shift reaction [1, 50, 51].

8. Conclusions

First we have shown that the feedback of the physical chemistry is necessary to make more reliable and safer the treatment of water and aqueous solutions; they are used on a large scale in the power cycle. We have focused on molecular-level information on the behaviors of hot water under supercritical conditions. The high-temperature NMR probe employed for the microscopic studies has been described in brief together with further improvements. Now it is possible to use multinuclear NMR probe instead of electric conductivity to obtain the mobility of ionic and nonionic species in aqueous solutions at high temperatures.

NMR spectroscopic study of hot water has clarified that there remain certain amount of hydrogen bonds in supercritical water, depending on the density; hydrogen bonds are sensitive to the density rather than the temperatures. Near the critical density at 400 °C, the number of hydrogen bonds per molecule is about two, although the fluctuations are huge. The dynamics of water rotation is accelerated to a large extent in supercritical water at 400 °C, compared with that of ambient water. The rotational correlation time is about 1 ps in ambient water, and it is reduced to several ten fs in supercritical water. The acceleration is induced by the breakage of the hydrogen bonds in the early decrease in the density due to the expansion. However, the correlation is not very sensitive to the density over a wide range near the critical density, probably due to the rapid motions of supercritical water molecules even in the associated state through hydrogen bonds.

A variety of weakly polar organic molecules begin to show new chemical reaction in hot water, because of the increased solubility and the increased stability of the transition state. The stabilization of the transition state of organics is accomplished not by the proton (hydroxide) generated by the autoprotolysis of hot water but by the neutral water molecules themselves. This is established by separating the rate constant due to the proton catalysis and that due to the neutral water. This might give us a hint to the corrosion mechanism in the power cycle.

We have discovered several new chemical reactions in supercritical water. (1) Rubbers can be cracked to paraffin [52]. (2) Dicholoromethane can be subjected to the self- and cross-disproportionations (bimolecular oxidation-reduction) forming alcohol and acid. (3) Dichloromethane (a formaldehyde producer) can be transformed into glycolic acid, forming a new C-C bond. (4) Formic acid can be used as a chemical tank for hydrogen fuel technology. (5) Supercritical water is useful for the preferential H/D exchange reaction without catalyst [53]. It is evidenced as an intermediate of the water-gas-shift reaction. Hot water clusters play a key role in controlling the discovered organic reaction pathways. Thus water can be regarded as a strong microscopic catalyst.

Acknowledgments

This work was supported by the Grant-in-Aid for Scientific Research 15205004 from Japan Society for the Promotion of Science and by the Grant-in-Aid for Creative Scientific Research 13NP0201 and the Grant-in-Aid for Scientific Research on Priority Area 15076205 from the Ministry of Education, Culture, Sports, Science and Technology, Japan.

References and Notes

[1] K. Yoshida, C. Wakai, N. Matubayasi, and M. Nakahara, *J. Phys. Chem. A*, **108**, 7479 (2004).
[2] Y. Nagai, N. Matubayasi, and M. Nakahara, *J. Phys. Chem. A*, in press (2005), Part 2.
[3] M. Nakahara, *Netsusokutei*, **31**, 14 (2004), in Japanese.
[4] M. Nakahara and N. Matubayasi, *Bunseki*, 29 (2004),

in Japanese.
[5] M. Nakahara, *Nippon Gomu Kyokaishi*, **77**, 365 (2004), in Japanese.
[6] M. Nakahara and J. Osugi, *Rev. Phys. Chem. Jpn*., **50**, 66 (1980).
[7] M. Nakahara, N. Takisawa, and J. Osugi, *J. Phys. Chem*., **85**, 112 (1981).
[8] N. Takisawa, J. Osugi, and M. Nakahara, *J. Phys. Chem*., **85**, 3582 (1981).
[9] M. Nakahara, T. T örök, N. Takisawa, and J. Osugi, *J. Chem. Phys*., **76**, 5145 (1982).
[10] N. Takisawa, J. Osugi, and M. Nakahara, *J. Chem. Phys*. **77**, 4717 (1982).
[11] N. Takisawa, J. Osugi, and M. Nakahara, *J. Chem. Phys*., **79**, 2591 (1983).
[12] M. Nakahara, *J. Phys. Chem*., **88**, 2138 (1984).
[13] M. Nakahara, M. Zenke, M. Ueno, and K. Shimizu, *J. Chem. Phys*., **83**, 280 (1985).
[14] K. Ibuki and M. Nakahara, *J. Chem. Phys*., **84**, 2776 (1986).
[15] K. Ibuki and M. Nakahara, *J. Chem. Phys*., **84**, 6979 (1986).
[16] M. Nakahara and K. Ibuki, *J. Phys. Chem*., **90**, 3026 (1986).
[17] K. Ibuki and M. Nakahara, *J. Phys. Chem*., **90**, 6362 (1986).
[18] M. Nakahara and K. Ibuki, *J. Chem. Phys*., **85**, 4654 (1986).
[19] K. Ibuki and M. Nakahara, *J. Chem. Phys*., **85**, 7312 (1986).
[20] M. Nakahara and M. Zenke, *Bull. Chem. Soc. Jpn*., **60**, 493 (1987).
[21] K. Ibuki and M. Nakahara, *J. Phys. Chem*., **91**, 1864 (1987).
[22] K. Ibuki and M. Nakahara, *J. Phys. Chem*., **91**, 4411 (1987).
[23] K. Ibuki and M. Nakahara, *J. Phys. Chem*., **91**, 4414 (1987).
[24] K. Ibuki, M. Ueno, and M. Nakahara, *J. Phys. Chem. B*, **104**, 5139(2000).
[25] K. Ibuki, M. Ueno, and M. Nakahara, *J. Mol. Liquids*, **98-99**, 129 (2002).
[26] M. Kubo, R. M. Levy, P. J. Rossky, N. Matubayasi, and M. Nakahara, *J. Phys. Chem. B*, **106**, 3979 (2002).
[27] N. Matubayasi, C. Wakai, and M. Nakahara, *Phys. Rev. Lett*., **78**, 2573 (1997).
[28] N. Matubayasi, C. Wakai, and M. Nakahara, *J. Chem. Phys*., **107**, 9133 (1997).
[29] K. Yoshida, C. Wakai, N. Matubayasi, and M. Nakahara, to be submitted.
[30] K. Yoshida, C. Wakai, N. Matubayasi, and M. Nakahara, The 44th Annual Meeting of the Japan Society of High-Pressure Science and Technology (Yokohama, 2003), Abstract, p 93.
[31] M. Nakahara, T. Yamaguchi, and H. Ohtaki,, *Recent Res. Devel. in Phys. Chem*., **1**, 17 (1997).
[32] P. Postorino, R. H.Tromp, M. A. Ricci, A. K. Soper, and G. W. Neilson, *Nature*, **366**, 668 (1993).
[33] N. Matubayasi, C. Wakai, and M. Nakahara, *J. Chem. Phys*., **110**, 8000 (1999).
[34] M. M. Hoffmann and M. K. Conradi, *J. Am. Chem. Soc.*, **119**, 3811 (1997).
[35] Y. Takebayashi, S. Yorita, T. Sugata, M. Ohtake, and M. Nakahara, *J. Chem. Phys*., **120**, 6100 (2004).
[36] N. Matubayasi, N. Nakao, and M. Nakahara, *J. Chem. Phys*., **114**, 4107 (2001).
[37] W. J. Lamb and J. Jonas, *J. Chem. Phys*. **74**, 913 (1981).
[39] Y. Nagai, N. Matubayasi, and M. Nakahara, *Bull. Chem. Soc. Jpn*. **77**, 691 (2004).
[38] Y. Nagai, S. Morooka, N. Matubayasi, and M. Nakahara, *J. Phys. Chem. A*, **108,** 11635 (2004).
[40] K. S. Pitzer (Eds), "Activity coefficients in electrolyte solutions", 2nd ed., CRC Press, Inc., Boca Raton (1991). .
[41] Y. Tsujino, C. Wakai, N. Matubayasi, and M. Nakahara, *Chem. Lett*. **28**, 287 (1999).
[42] Y. Nagai, C. Wakai, N. Matubayasi, and M. Nakahara, *Chem. Lett*. **32**, 310 (2003).
[43] Y. Nagai, N. Matubayasi, and M. Nakahara, *Chem. Lett*. **33**, 622 (2004).
[44] C. Wakai, S. Morooka, N. Matubayasi, and M. Nakahara, *Chem. Lett.,* **33,** 302 (2004).
[45] S. Morooka, C. Wakai, N. Matubayasi, and M. Nakahara, *Chem. Lett.* **33**, 624 (2004).
[46] Y. Nagai, N. Matubayasi, and M. Nakahara, *J. Phys. Chem. A*, in press (2005), Part 1.
[47] N. Matubayasi and M. Nakahara, *J. Chem. Phys*., **113**, 6070 (2000).
[48] N. Matubayasi and M. Nakahara, *J. Chem. Phys*., **117**, 3605 (2002).
[49] N. Matubayasi and M. Nakahara, *J. Chem. Phys*., **119**, 9686 (2003).
[50] H. Takahashi, N. Matubayasi, M. Nakahara, and T. Nitta, *J. Chem. Phys.,* **121,** 3989 (2004).
[51] N. Matubayasi and M. Nakahara, *J. Chem. Phys*., **122**, 074509 (2005).
[52] M. Nakahara, T. Tennoh, C. Wakai, E. Fujita, and H. Enomoto, *Chem. Lett*., **26**, 163 (1997).
[53] M. Kubo, T. Takizawa, C. Wakai, N. Matubayasi, and M. Nakahara, *J. Chem. Phys.,* **121,** 960 (2004).